



## Physics with jets in $p\bar{p}$ collisions

W. T. Giele

*Fermi National Accelerator Laboratory, P. O. Box 500,  
Batavia, IL 60510, U.S.A.*

and

E. W. N. Glover

*Physics Department, University of Durham,  
Durham DH1 3LE, England*

June 26, 1995

### Abstract

We discuss the possibilities for extracting information on the parton density functions and the strong coupling constant from one- and two-jet events at the Fermi-lab TEVATRON. First we study the inclusive two-jet triply differential cross section  $d^3\sigma/dE_T d\eta_1 d\eta_2$ . Different  $\eta_1$  and  $\eta_2$  pseudorapidity regions are directly related to the parton momentum fractions at leading order and the shape of the triply differential distribution at fixed transverse energy  $E_T$  is a particularly powerful tool for constraining the parton distributions at small to moderate  $x$  values. Second, we consider the one-jet inclusive transverse energy distribution where there is impressive agreement between theory and experiment over a wide range of transverse energy. By equating the next-to-leading order theoretical prediction for a given set of input parton densities with the published CDF data, the evolution of the strong coupling constant at scale  $\mu$  can be studied between  $\mu \sim 50$  GeV and  $\mu \sim 400$  GeV. This evolution is in agreement with QCD and corresponds to  $\alpha_s(M_Z) = 0.121$  for the MRSA parameterisation.



One- and two-jet production in hadron collisions occurs when two partons from the incident hadrons undergo a hard pointlike interaction and scatter at relatively large angles. The cross section depends on the non-perturbative probability of finding a particular parton inside the parent hadron, the strong coupling constant and the dynamics of the hard scattering which can be calculated perturbatively. In many cases there is excellent qualitative agreement between the observed jet cross sections and perturbative QCD calculations at next-to-leading order based on input parton density functions and strong coupling constant derived from lower energy experiments. For example, the single jet inclusive transverse energy distribution is well described over eight orders of magnitude. With this qualitative agreement in mind, we might expect to be able to use the theoretical description of the hard scattering to extract the input parameters such as the distribution of partons in the proton from the data. This would be particularly interesting since gluon scattering plays a very important role in two jet production, and it may be possible to probe the gluon density in a more direct way than is possible in deeply inelastic scattering or in Drell-Yan processes. In this talk, we briefly discuss how such determinations might be attempted at the TEVATRON using the inclusive two-jet cross section and the single-jet inclusive transverse energy distribution.

In comparing theory with experiment, we use the  $\mathcal{O}(\alpha_s^3)$  Monte Carlo program JETRAD for one, two and three jet production based on the one-loop  $2 \rightarrow 2$  and the tree level  $2 \rightarrow 3$  parton scattering amplitudes [1] described in ref. [2]. This program uses the techniques of refs. [3, 4] to cancel the infrared and ultraviolet singularities thereby rendering the  $2 \rightarrow 2$  and  $2 \rightarrow 3$  parton processes finite and amenable to numerical computation. The parton four momenta are then passed through the parton level equivalent of the standard ‘Snowmass’ cone algorithm [5] with  $\Delta R = 0.7$  to determine the one, two and three jet cross sections according to the experimental cuts. Throughout, we shall evaluate the cross section at a renormalisation and factorisation scale  $\mu = E_{T1}$ , where  $E_{T1}$  is the transverse energy of the hardest jet in the event.

The inclusive two-jet cross section can be described in terms of variables most suited to the geometry of the detector; the transverse energy of the leading jet,  $E_T = E_{T1}$ , and the pseudorapidities of the two leading jets,  $\eta_1$  and  $\eta_2$ . Recently, the D0 collaboration has presented a preliminary measurement of  $d^3\sigma/dE_T d\eta_1 d\eta_2$  [6, 7, 8] as a function of  $\eta_1$  and  $\eta_2$  at fixed  $E_T$ . At leading order,  $\eta_1$  and  $\eta_2$  are directly related to the parton momentum fractions  $x_1, x_2$ , so that this corresponds to a measurement of  $d^2\sigma/dx_1 dx_2$ . Of course, beyond leading order, the parton momentum fractions are only approximately determined by the transverse energies and pseudorapidities of the two leading jets.

For the typical transverse energies probed by CDF and D0,  $\mathcal{O}(30 - 50 \text{ GeV})$ , the values of  $x$  range between  $x_1 \sim 4E_T^2/s \sim 10^{-3}$ ,  $x_2 \sim 1$  for  $\eta_1 \sim \eta_2 \sim 4$  to  $x_1 \sim x_2 \sim 2E_T/\sqrt{s} \sim 0.05$  for  $\eta_1 \sim \eta_2 \sim 0$ . This covers both the small  $x$  region where gluons with singular behaviour ( $xg(x) \sim x^{-\lambda}$  and  $\lambda \sim 0.3 - 0.5$ ) dominate and the intermediate  $x$  region where the momentum sum rule ensures that the less singular gluon distributions carry a larger

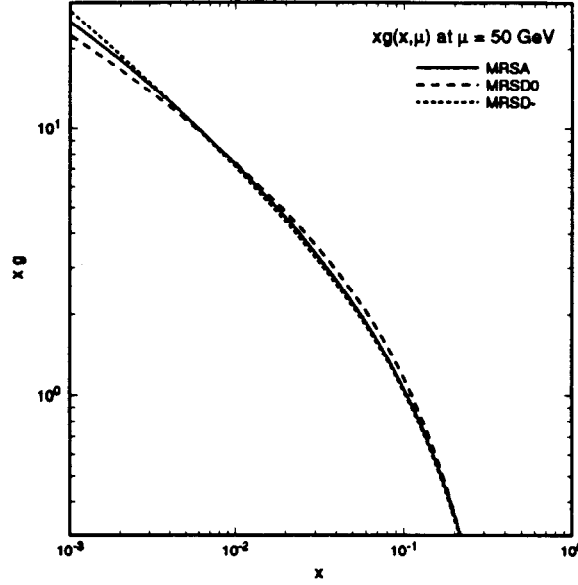


Figure 1: The momentum fraction  $xg(x, \mu)$  carried by the gluon for  $\mu = 50$  GeV for the MRSA, MRSD0 and MRSD- parton densities.

fraction of the momentum. This is illustrated in Fig. 1 where  $xg(x)$  is shown for the MRSA parameterisation [9] corresponding to  $\lambda \sim 0.3$  as favoured by the HERA data. To guide the eye, we also show the older pre-HERA MRSD0 and MRSD- [10] distributions with a flat ( $\lambda \sim 0$ ) and singular ( $\lambda \sim 0.5$ ) behaviour respectively.

Both the CDF [11] and D0 [6, 7, 8] collaborations have focused on particular slices of the triply differential distribution. D0 study the signed pseudorapidity distribution which amounts to taking two strips of the  $\eta_1 - \eta_2$  plane for a fixed transverse energy interval and combining them in reverse directions. The pseudorapidity of the leading jet is constrained to lie in the range  $|\eta_1|_{\min} < |\eta_1| < |\eta_1|_{\max}$  and the distribution is plotted as a function of  $|\eta_2| \text{sign}(\eta_1 \eta_2)$ ,

$$\frac{d\sigma}{d|\eta_2| \text{sign}(\eta_1 \eta_2)} \equiv \frac{1}{\Delta E_T} \int_{E_{T\min}}^{E_{T\max}} dE_T \frac{1}{2\Delta\eta_1} \left( \int_{|\eta_1|_{\min}}^{|\eta_1|_{\max}} d\eta_1 \frac{d^3\sigma}{dE_T d\eta_1 d\eta_2} - \int_{-|\eta_1|_{\max}}^{-|\eta_1|_{\min}} d\eta_1 \frac{d^3\sigma}{dE_T d\eta_1 d\eta_2} \right),$$

where  $\text{sign}(\eta_1 \eta_2) = -1$  if  $\eta_1$  and  $\eta_2$  have opposite sign and  $+1$  if they have the same sign. Positive values of  $|\eta_2| \text{sign}(\eta_1 \eta_2)$  correspond to same-side dijet events, while negative values are associated with opposite-side events. Fig. 2(a) shows the preliminary data for  $45 \text{ GeV} < E_T < 55 \text{ GeV}$  and  $0.0 < |\eta_1| < 0.5$ . In the small  $|\eta_2|$  region this is sensitive to  $x \sim 0.05$ . The next-to-leading order QCD predictions [12] are also shown. Although the errors are large and the overall normalisation is uncertain, there is a slight preference for the MRSD0 parameterisation indicating that perhaps more gluons are needed in the intermediate  $x$  range than suggested by the low  $x$  data from HERA combined with the momentum sum rule.

The interpretation of D0 signed distribution measurement will ultimately hinge on the

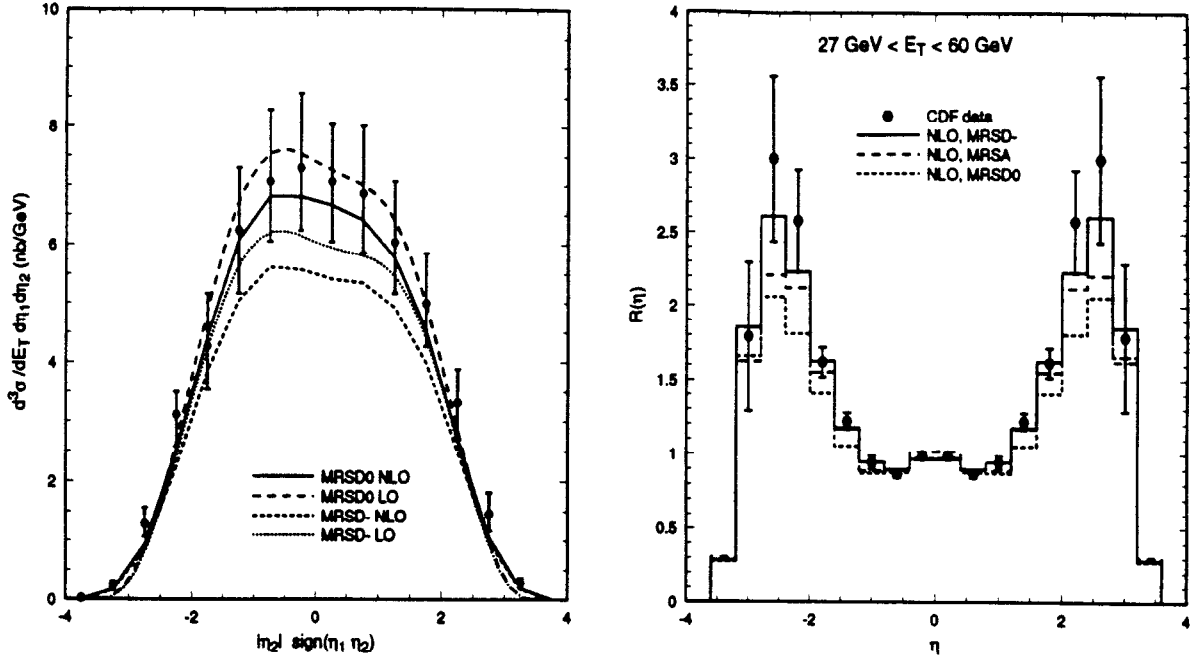


Figure 2: The next-to-leading order (NLO) predictions for (a) the signed pseudorapidity distribution for  $45 \text{ GeV} < E_T < 55 \text{ GeV}$ ,  $0.0 < |\eta_1| < 0.5$  and (b) the SS/OS ratio  $R(\eta)$  for  $27 \text{ GeV} < E_T < 60 \text{ GeV}$  for the MRSD- (solid) and MRSD0 (dashed) parton distributions. The preliminary experimental results from [6] and [11] are also plotted.

absolute normalisation of the cross section. To circumvent this problem the CDF collaboration has considered a ratio, that of same-side (SS) to opposite-side (OS) cross sections [11]. For the same-side cross section, both jets have roughly the same pseudorapidity, while in the opposite-side cross section the jets are required to have roughly equal, but opposite pseudorapidities,

$$\begin{aligned} \sigma_{SS}(\eta) \Big|_{E_{T\min} < E_T < E_{T\max}} &= \int_{\eta-\Delta\eta}^{\eta+\Delta\eta} d\eta_1 \int_{\eta-\Delta\eta}^{\eta+\Delta\eta} d\eta_2 \int_{E_{T\min}}^{E_{T\max}} dE_T \frac{d^3\sigma}{dE_T d\eta_1 d\eta_2}, \\ \sigma_{OS}(\eta) \Big|_{E_{T\min} < E_T < E_{T\max}} &= \int_{\eta-\Delta\eta}^{\eta+\Delta\eta} d\eta_1 \int_{-\eta-\Delta\eta}^{-\eta+\Delta\eta} d\eta_2 \int_{E_{T\min}}^{E_{T\max}} dE_T \frac{d^3\sigma}{dE_T d\eta_1 d\eta_2}. \end{aligned}$$

From these cross sections we form the SS/OS ratio,

$$R_{SS/OS}(\eta) \Big|_{E_{T\min} < E_T < E_{T\max}} = \frac{\sigma_{SS}(\eta) \Big|_{E_{T\min} < E_T < E_{T\max}}}{\sigma_{OS}(\eta) \Big|_{E_{T\min} < E_T < E_{T\max}}},$$

with the advantage that a large part of the experimental and theoretical uncertainties cancel. This ratio loses information on the parton densities in the central region where  $\eta_1 \sim \eta_2 \sim 0$ . However, at larger pseudorapidities it is sensitive to smaller  $x$  values  $x \sim 4E_T^2/s$ . Fig. 2(b) shows the preliminary data for  $27 \text{ GeV} < E_T < 60 \text{ GeV}$ . At  $\eta \sim 2.6$ , this probes  $x \sim 0.001$ . The next-to-leading order QCD predictions [13] for which the renormalisation scale dependence is small are also shown. Although the experimental errors are large, there is now

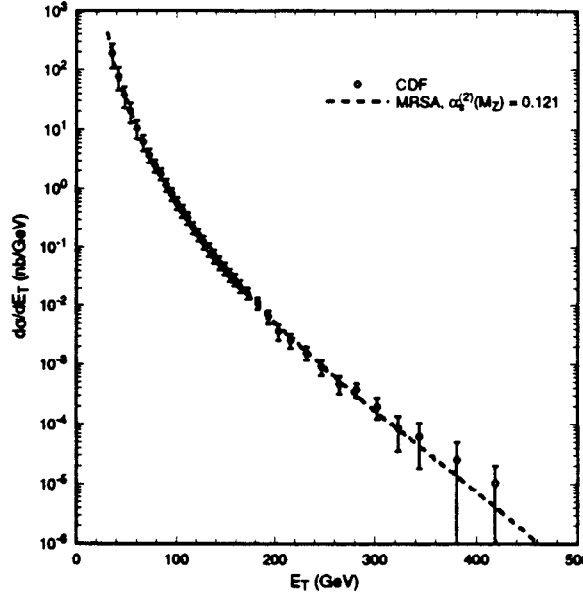


Figure 3: The next-to-leading order prediction for the single jet inclusive transverse energy distribution for the MRSA parton distributions and  $\alpha_s^{(2)}(M_Z) = 0.121$ . The CDF data from [16] is also shown.

a slight preference for the MRSD- parameterisation indicating that perhaps more gluons are needed in the low  $x$  range than currently preferred by HERA.

We now consider what information on the strong coupling constant  $\alpha_s$  can be gleaned from the single jet transverse energy distribution. Up to  $\mathcal{O}(\alpha_s^3)$ , this is given by,

$$\frac{d\sigma}{dE_T} = \left(\frac{\alpha_s(\mu)}{2\pi}\right)^2 A + \left(\frac{\alpha_s(\mu)}{2\pi}\right)^3 \left[ B + 2b_0 \log\left(\frac{\mu^2}{E_T^2}\right) \right], \quad (1)$$

where  $\mu$  is the renormalisation scale,  $b_0 = (33 - 2n_f)/6$  and the next-to-leading order coefficient  $B$  has been known for some time [14, 15]. Fig. 3 shows the excellent agreement between next-to-leading order QCD and the published CDF data [16] over eight orders of magnitude. We might therefore hope to use this agreement to extract information on the strong coupling. However, both  $A$  and  $B$  depend on the factorisation scale  $\mu_F$  and the input parton densities (which themselves implicitly depend on  $\alpha_s$ ). These dependences will ultimately form part of the theoretical error in measuring  $\alpha_s$  along with the usual renormalisation scale uncertainty. For a first look at what can be learned, we fix  $\mu_F = E_T$  and use the MRSA parameterisation of the parton densities, ignoring the value of  $\alpha_s$  it was derived from. We also fix the renormalisation scale to be the transverse energy of the jet,  $\mu = E_T$  and extract a value of  $\alpha_s(E_T)$  by solving Eq. 1 for each of the 38 data points, yielding in principle 38 separate measurements of  $\alpha_s$ .<sup>1</sup> This is shown in Fig. 4a along with the value

<sup>1</sup>A more careful analysis would require the experimental error to be resolved into a bin-by-bin error and a common systematic error.

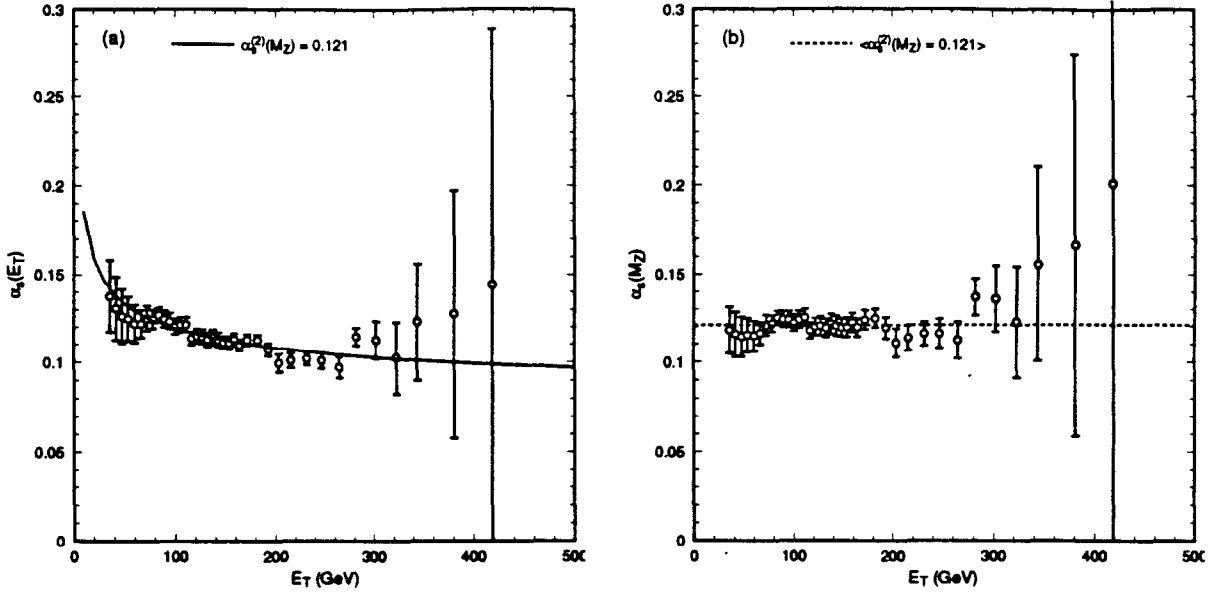


Figure 4: (a) The value of  $\alpha_s(E_T)$  extracted using the published CDF data [16] and Eq. 1 compared to the next-to-leading order evolution with  $\alpha_s(M_Z) = 0.121$  (solid) and (b) the value of  $\alpha_s(M_Z)$  obtained when evolving from  $\mu = E_T$  to  $\mu = M_Z$ .

of  $\alpha_s(E_T)$  obtained from  $\alpha_s^{(2)}(M_Z) = 0.121$  using the renormalisation group evolution. The running of the strong coupling is clear and is qualitatively in agreement with expectations.

We can take this one step further by using the renormalisation group equations to evolve the extracted value of  $\alpha_s(E_T)$  back to  $\mu = M_Z$  for each data point, yielding 38 estimates of  $\alpha_s(M_Z)$  as shown in Fig. 4b. The results are essentially independent of the  $E_T$  at which  $\alpha_s(M_Z)$  was extracted and the error weighted average is  $\langle \alpha_s(M_Z) \rangle = 0.121$ . This can be compared with the input value used in the parton distribution evolution of  $\alpha_s(M_Z) = 0.111$ . As mentioned earlier, the value of  $\alpha_s$  extracted in this way also depends on the choice of input parton densities. For the MRSD0 parameterisation, the same analysis gives  $\langle \alpha_s(M_Z) \rangle = 0.118$  while for the MRSD- set we find  $\langle \alpha_s(M_Z) \rangle = 0.123$ .

Clearly there is more work to be done in understanding both the theoretical and experimental error. However, the rewards of observing the evolution of the strong coupling over nearly an order of magnitude of scale in a single experiment would be considerable, particularly when we bear in mind that the current TEVATRON run should obtain 25 times more data than that analysed here. Similarly, one would expect that with the increase in statistics of the dijet data, it might be possible to track the high  $Q^2$  evolution by varying the transverse energy of the jet as well as providing a significant constraint on the parton distributions.

# Acknowledgements

We thank David Kosower for many valuable insights throughout a stimulating collaboration. EWNG gratefully acknowledges the financial support of the EC Human Capital and Mobility Network contract ERBCHRXCT930357.

# References

- [1] R. K. Ellis and J. Sexton, Nucl. Phys. **B269**, 445 (1986).
- [2] W. T. Giele, E. W. N. Glover and D. A. Kosower, Phys. Rev. Lett. **73**, 2019 (1994).
- [3] W. T. Giele and E. W. N. Glover, Phys. Rev. **D46**, 1980 (1992).
- [4] W. T. Giele, E. W. N. Glover and D. A. Kosower, Nucl. Phys. **B403**, 633 (1993).
- [5] See, for example, J.E. Huth *et al*, in Research Directions for the Decade, Proceedings of the 1990 Division of Particles and Fields Summer Study, Snowmass, 1990, edited by E.L. Berger (World Scientific, Singapore, 1992), p.134.
- [6] D0 Collaboration, presented by Harry Weerts, Ninth Topical Workshop on Proton – Anti-proton Collider Physics, Tsukuba, Fermilab preprint, FERMILAB-CONF-94/35-E.
- [7] D0 collaboration, presented by Freedy Nang, Eighth Meeting of the Division of Particles and Fields of the American Physical Society, Albuquerque, New Mexico, August 1994, Fermilab preprint FERMILAB-CONF-94-341-E.
- [8] D0 Collaboration, presented by T. Geld, this conference.
- [9] A. D. Martin, R. G. Roberts and W. J. Stirling, Durham preprint DTP/94/34.
- [10] A. D. Martin, R. G. Roberts and W. J. Stirling, Phys. Lett. **B306**, 145 (1993).
- [11] CDF Collaboration, F. Abe *et al*, Fermilab preprint, FERMILAB-CONF-93/203-E; CDF Collaboration, presented by Eve Kovacs, Eighth Meeting of the Division of Particles and Fields of the American Physical Society, Albuquerque, New Mexico, August 1994, Fermilab preprint FERMILAB-CONF-94/215-E.
- [12] W. T. Giele, E. W. N. Glover and D. A. Kosower, Fermilab preprint FERMILAB-PUB-94/382-T, to be published in Phys. Rev. **D**.
- [13] W. T. Giele, E. W. N. Glover and D. A. Kosower, Phys. Lett. **B339**, 181 (1994).
- [14] S. D. Ellis *et al.*, Phys. Rev. **D40**, 2188 (1989); Phys. Rev. Letts. **64**, 2121 (1990).

- [15] F. Aversa et al., Phys. Rev. Letts. **65**, 401 (1990); Z. Phys. **C49**, 459 (1991).
- [16] F. Abe et al., CDF Collab., Phys. Rev. Letts. **68**, 1104 (1992), Fermilab preprint FERMILAB-PUB-91-231-E.